Molecular Crystals and Liquid Crystals Science and Technology. Section A. Molecular Crystals and Liquid Crystals

Publication details, including instructions for authors and subscription information:
http://www.tandfonline.com/loi/gmcl19

Electronic Structures of Porphyrins and their Interfaces with Metals Studied by UV Photoemission

H. Ishii [a d], S. Hasegawa [a], D. Yoshimura [b], K. Sugiyama [b], S. Narioka [b], M. Sei [b], Y. Ouchi [b], K. Seki [b], Y. Harima [c] & K. Yamashita [c]

[a] Institute for Molecular Science, Myodaiji, Okazaki, 444, Japan

[b] Department of Chemistry, Faculty of Science, Nagoya University, Furo-cho, Chikusa-ku, Nagoya, 464-01, Japan

[c] Faculty of Integrated Arts and Sciences, Hirosima University, Kagamiyama, Higashi-Hiroshima, 724, Japan

[d] Department of Chemistry, Nagoya University

Version of record first published: 24 Sep 2006

To cite this article: H. Ishii, S. Hasegawa, D. Yoshimura, K. Sugiyama, S. Narioka, M. Sei, Y. Ouchi, K. Seki, Y. Harima & K. Yamashita (1997): Electronic Structures of Porphyrins and their Interfaces with Metals Studied by UV Photoemission, Molecular Crystals and Liquid Crystals Science and Technology. Section A. Molecular Crystals and Liquid Crystals, 296:1, 427-444

To link to this article: http://dx.doi.org/10.1080/10587259708032338

Mol. Cryst. Liq. Cryst., 1997, Vol. 296, pp. 427–444
Reprints available directly from the publisher
Photocopying permitted by license only

ELECTRONIC STRUCTURES OF PORPHYRINS AND THEIR INTERFACES WITH METALS STUDIED BY UV PHOTOEMISSION

HISAO ISHII* AND SHINJI HASEGAWA
Institute for Molecular Science, Myodaiji, Okazaki 444, Japan
DAISUKE YOSHIMURA, KIYOSHI SUGIYAMA, SATORU NARIOKA, MASAKI SEI, YUKIO OUCHI, AND KAZUHIKO SEKI
Department of Chemistry, Faculty of Science, Nagoya University,
Furo-cho, Chikusa-ku, Nagoya 464-01, Japan
YUTAKA HARIMA, AND KAZUO YAMASHITA
Faculty of Integrated Arts and Sciences, Hirosima University,
Kagamiyama, Higashi-Hiroshima 724, Japan

ABSTRACT The electronic structures of porphyrins and their interfaces with metals were investigated by UV photoemission spectroscopy (UPS). The UPS spectral features of porphine, 5,10,15,20-tetraphenylporphynatozinc(II) (ZnTPP), 5,10,15,20-tetra(4-pyridyl)porphyrin ($H_2T(4\text{-Py})P$) and 5,10,15,20-tetraphenylporphyrin (H_2TPP) could be assigned by comparison with MOPAC PM3 calculations. The electronic structures of the porphyrins can be regarded as the superposition of those of porphine and the substituents. The UPS results for ZnTPP/metal (Mg, Al, Ag, Au) interfaces indicated that the energies of the levels of ZnTPP relative to the Fermi level of substrate metals could be expressed as linear functions of the work function of metals with a shift of the vacuum level at interface. The slope of the linear functions was about unity. This indicates that the energy levels of ZnTPP are fixed to the vacuum level of substrate metal with constant interfacial dipole. The level positions of ZnTPP at the interface exhibited drastic change by exposure to oxygen. This change could be explained by the change of the work function of metal surface upon oxidization. For $H_2T(4\text{-Py})P$ and H_2TPP/metal (Mg, Ag, Au) interfaces, similar linearity was observed between the energy levels of porphyrin and the work function of metal with the slope of much smaller than unity. This deviation of the slope from unity might be explained by the existence of interface state. These findings require the modification of the traditional concept of a common vacuum level at organic/metal interface. The relation between the observed electronic structures and the conduction type of the porphyrins are also discussed.

Keywords: photoemission, porphyrin, porphine, electronic structure, interface

* On leave from Department of Chemistry, Nagoya University.

INTRODUCTION

Recently various organic semiconductors have been extensively studied in relation to electronic devices such as transistors, photovoltaic cells, and electroluminescent devices[1]. The various properties of organic semiconductors have often been discussed in analogy with inorganic semiconductors. Among such analogies, there are two important issues for understanding and refining the performance of such devices: one is the mechanism of the energy level alignment at organic/metal interface and the other is the classification of the conducting type of organic semiconductors.

Since the functions of organic devices often appear at the interfaces between organic semiconductors and metal electrodes, the energy positions of the frontier orbitals of organic semiconductors relative to the Fermi level of a metal are crucial to the property of the interface such as carrier injection and rectification. However, there have been few direct observations of the interfacial electronic structures with microscopic method[2,3,4,5]. So far it has mostly been estimated by lining up separately observed electronic energy levels of the two components, using the traditional models assuming either that (a) vacuum level alignment occurs at the interface and energy levels in space charge layer bend to achieve Fermi level alignment, which corresponds to a traditional model of inorganic-semiconductor/metal interface (Fig.1a) (Schottky-Mott rule[6]), or that (b) the vacuum level of an organic layer coincides with that of metal without band bending which coincides with the traditional model of insulator/metal interface (Fig.1b). However, the validity of these traditional models for organic-semiconductor/metal interface has not yet been well clarified. Especially, the concept of a common vacuum level at the interface, which has been intuitively assumed in both the above models, should be experimentally examined.

The conduction type of organic semiconductors is also crucial for the interfacial properties. Phenomenologically, various organic semiconductors have been classified by the conduction type such as *p-type and n-type*. This classification is based on the analogy with inorganic semiconductors. In the case of inorganic semiconductors, the conduction type is determined by (i) the type of the major carrier and (ii) the position of the Fermi level in the gap. Unfortunately, it is not easy to directly decide the type of the major carrier and Fermi level position of organic semiconductors because of their low carrier density. Instead, the rectification properties and the photocurrent direction of the interface with a metal electrode has often been applied to determine the conduction type of organic semiconductors[7,8,9]. However, the mechanism of the classification is not well understood. Recently, a strong correlation between the first ionization potentials and the conduction type was observed for phthalocyanines whose

conducting type can be changed from *p*-type to *n*-type by addition of electron-withdrawing substitutions to the central ring[10]. However, the position of the frontier orbital at the interface is expected to have more essential relation to the conducting type than the ionization potential as a bulk property, since the conducting type of an organic semiconductor is judged by the electric properties of the interface with a metal electrode. Thus the difference in the interfacial electronic structure between "*p*-type" and "*n*-type" materials should be investigated.

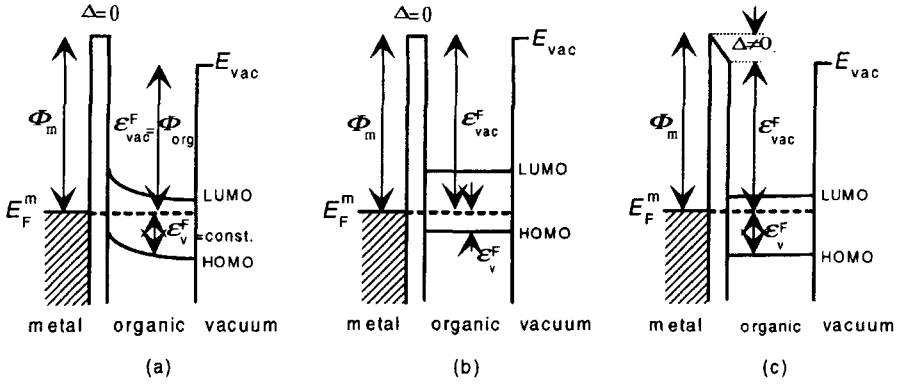

FIGURE 1. The energy diagrams at organic/metal interface. (a) Fermi level alignment case (Schottky-Mott rule), (b) vacuum level alignment case, (c) presently observed alignment for porphyrins. It should be noted that the dashed lines in (b) and (c) do not denote the Fermi level of the organic solids but simply indicates the location of the Fermi level of the metal. Φ_m and Φ_{org} denote the work functions of the metal and the organic solid, respectively. $\varepsilon_{vac}{}^F$ and $\varepsilon_v{}^F$ represent the energy of the vacuum level and the top of the occupied states of the organic solid relative to the Fermi level of the metal, respectively. Δ is defined as the shift of the vacuum level at the interface.

In this work, we report our recent studies on the electronic structures of porphyrin/metal interfaces by UV photoemission spectroscopy (UPS). These interfaces have attracted much attention in relation to organic solar cells[8]. The conduction type of porphyrins can be changed from *p*-type to *n*-type by peripheral substitution[8]. Thus these compounds are suitable to examine the above issues. We measured UPS spectra of 5,10,15,20-tetraphenylporphinatozinc(II) (ZnTPP), 5,10,15,20-tetraphenylporphyrin

(H_2TPP), and 5,10,15,20-tetra(4-pyridyl)porphyrin (H_2T(4-Py)P) as well as porphine which is the central part of the porphyrins. The chemical structures are shown in Figure 2. We first discuss the change of the bulk electronic sturctures of the porphyrins by the substitution. Second we describe the UPS results on the interfacial electronic structures and discuss the energy level alignment at the interface, including the effect of oxygen on the porphyrin/metal interfaces. Finally, the relation between the interfacial electronic structure and the conduction type is discussed.

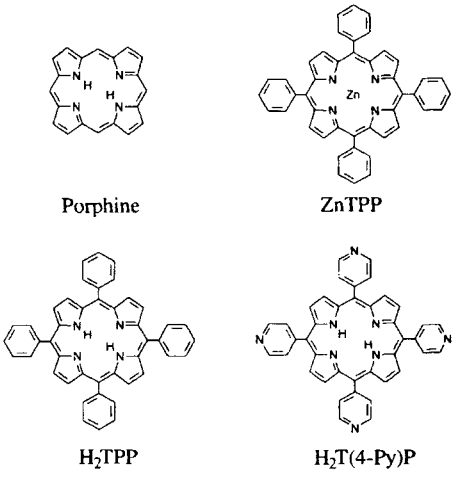

FIGURE 2. The chemical structure of porphine, 5,10,15,20-tetraphenyl-porphynatozinc (ZnTPP), 5,10,15,20-tetra-phenylporphyrin (H_2TPP), and 5,10,15,20-tetra(4-pyridyl)porphyrin (H_2T(4-Py)P).

EXPERIMENTAL

ZnTPP, H_2TPP, H_2T(4-Py)P and porphine were purchased from Strem Chemical, Tokyo Chemical Industry, Aldrich Chemical, and SIGMA Chemical, respectively. The samples of the porphyrins were purified by two times of vacuum sublimation. Before the vacuum sublimation, ZnTPP was purified by the treatment with 2,3-dichloro-4,5-dicyano-*p*-benzoquinone(DDQ)[11]. No purification treatment was performed for the sample of porphine due to the limited amount of available sample. Its purity was ca. 85% according to the supplier. Since vacuum deposition often has the effect of sample purification and we discarded the initial subliming fraction before starting the sample deposition, the purity of the UPS specimen might be higher than this.

UPS spectra were measured by using angle-resolving UPS system at the beamline 8B2 of UVSOR at Institute for Molecular Science[12]. We used four metals (Mg, Al,

Ag, Au) as substrate material, which were vacuum evaporated (30 nm thick) on Mo plates. Sample thin films were prepared by vacuum deposition on these substrates in a newly constructed preparation chamber equipped with an evaporation source surrounded by a liquid-nitrogen-cooled shroud. The base pressure was $1x10^{-10}$ Torr and the working pressure during evaporation was less than $2x10^{-9}$ Torr, which enabled us to suppress surface contamination during the evaporation. The UPS spectra were measured at the photon energy of 40eV with a concentric hemispherical analyzer with a total energy resolution of 0.2eV as judged from the Fermi edge of gold. The incident angle of photon was 40° relative to surface normal and electron was detected in normal emission for all the UPS measurements. The photon intensity was reduced by an appropriate mesh to keep the sample photocurrent less than 15pA, in order to avoid any energy shift of the spectrum due to sample charging or surface photovoltaic effect. The work functions of the samples were determined by the low energy cutoff of the UPS spectra measured with biasing the sample at -5 V for ensuring that the cutoff is not determined by the spectrometer work function but the sample work function. Since the value of the photon energy contained a small ambiguity of a few tenths of eV, we calibrated the obtained work functions by the reported work function of polycrystalline Ag of 4.3 eV[13]. Fortunately, this ambiguity of photon energy does not affect the following discussion, since the relative value is critical.

The MOPAC program developed by Stewart[14] was used for the PM3 calculations[15] for the assignment of the observed UPS spectra. The simulated spectra were obtained by broadening the delta function located at each orbital energy with a Gaussian function without correction for cross-section effects. The width of the Gaussian was chosen to be 0.6 eV in order to take account of the resolution of the UPS system and the solid-state spectral broadening[16]. No contraction of the energy scale was performed to fit the simulated spectrum to the observed UPS spectrum.

RESULTS AND DISCUSSION

(a) Bulk electronic structures of porphine and porphyrins

In Figure 3, we show the UPS spectrum of a porphine film (30nm thick) deposited on Ag/Mo substrate. Since the film thickness is much larger than the probing depth of UPS measurement (ca. 1nm for hν=40 eV), the UPS spectrum reflects the bulk electronic structure. The abscissa is the electron binding energy relative to the Fermi level of the substrate. In order to assign the spectral features, UPS spectrum of porphine in gas phase (Fig.3(a))[17] and simulated spectrum by MOPAC PM3 MO

calculation, together with each orbital energy marked by a vertical line, are also shown in Fig. 3. Although the UPS spectrum of porphine in solid phase has already been reported[18], it did not correspond to the gas phase spectrum. In particular, there seems to be no feature corresponding to peak A in the previous report. From good correspondence among the spectra shown in the figure, the present spectrum seems to be more reliable. The present PM3 calculation gives qualitatively similar results to those of the previous works by VEH[19], CNDO/S3[18], and ab initio[20,21]methods. From comparison with our PM3 calculation, we can assign the spectral features in solid phase spectrum (Fig.3b): peak A corresponds to the electron emission from the HOMO (a_u) and the next-HOMO (b_{1u}). Peaks B and C are due to π and σ orbitals delocalized over the molecule, and peaks D and E are assigned to the MOs derived from carbon 2s orbitals.

In Figures 4(b) and 4(c), the UPS spectra of ZnTPP for hν=40eV and 60eV are shown, respectively. For the assignment of the spectral features, the UPS of benzene[22] in gas phase (Fig.4(e)), that of porphine in solid phase(Fig.4(d)), and the simulated

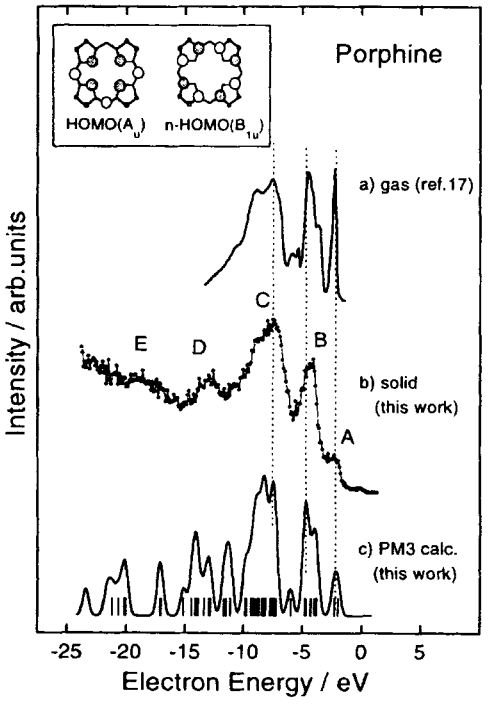

FIGURE 3.
UPS *spectra of* porphine. (a) gas-phase spectrum at hν=21.2eV [17],
(b) solid porphine at hν=40eV, (c) simulated spectrum by MOPAC PM3 calculation . Each vertical line indicates the respective orbital energy.

spectrum of ZnTPP by PM3 MO calculation (Fig.4(a)) are also shown. As seen in Figures 4(b) and 4(c), the peak at around 11.3eV becomes enhanced with increasing the photon energy from 40 eV to 60 eV. This can be explained by the resonance enhancement of the zinc 3d photoionization cross section which was reported for zinc phthalocyanine[23]. The spectra of porphine and benzene were aligned to those of ZnTPP at the C2s peaks. The simulated spectrum was shifted to get a better fit around the uppermost valence region. As seen in the figure, the spectrum of ZnTPP corresponds well to the superposition of those of the porphine, benzene (substituents) and zinc 3d (central-metal). This indicates that the valence electronic structure of ZnTPP can be regarded as a superposition of those of constituents parts. The uppermost valence electronic structure (peak A), which dominates the various properties of ZnTPP, can be attributed to nearly degenerate two π orbitals which correspond to a_u and b_{1u} orbitals of porphine by comparison with PM3 calculation.

The UPS spectra of the other porphyrins give similar results. Figures 5 and 6 show the UPS spectra of H_2TPP(Fig.5(b)) and H_2T(4-Py)P(Fig.6(b)) together with those of porphin and the substituents (benzene[22] for H_2TPP, and pyridine[24] for H_2T(4-Py)P). As in the case of ZnTPP, the valence electronic structures of the porphyrins correspond to the superposition of the constituent parts.

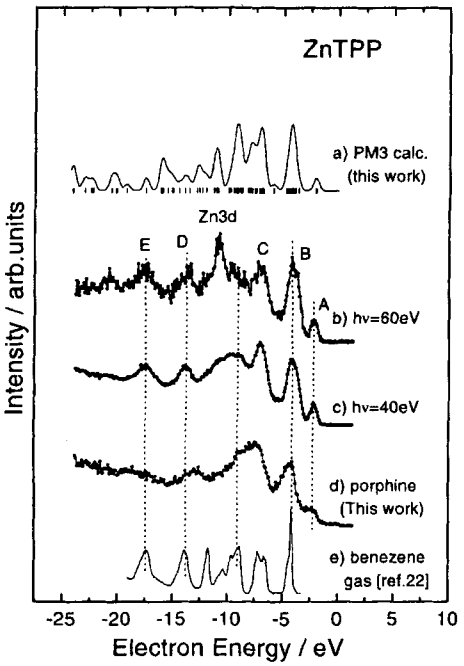

FIGURE 4.
UPS spectra of ZnTPP.
(a) simulated spectrum by MOPAC PM3 calculation. Each vertical line indicates respective orbital energy,
(b) solid ZnTPP at hv=60eV,
(c) solid ZnTPP at hv=40eV,
(d) solid porphine at hv=40eV,
(e) gas-phase benzene[22].

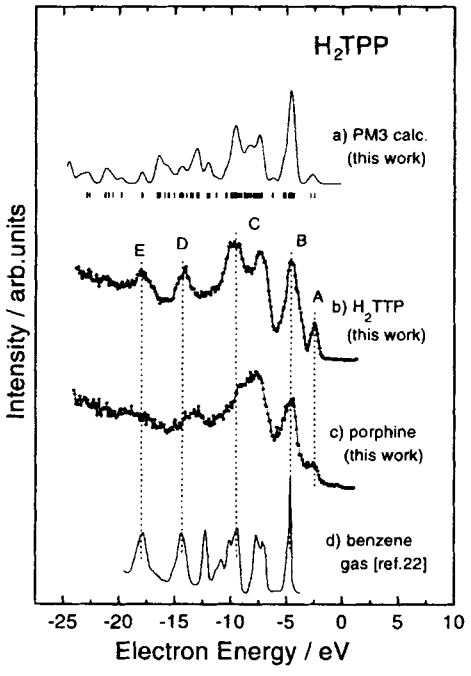

FIGURE 5.
UPS spectra of H_2TPP.
(a) simulated spectrum by MOPAC PM3 calculation. Each vertical line indicates respective orbital energy, (b) solid H_2TPP at hν=40eV,
(c) solid porphine at hν=40eV,
(d) gas-phase benzene[22].

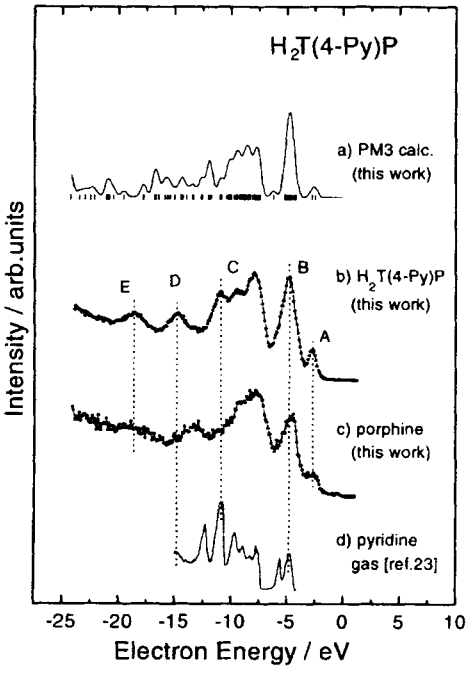

FIGURE 6.
UPS spectra of $H_2T(4\text{-}Py)P$.
(a) simulated spectrum by MOPAC PM3 calculation. Each vertical line indicates respective orbital energy,
(b) solid $H_2T(4\text{-}Py)P$ at hν=40eV,
(c) solid porphine at hν=40eV,
(d) gas-phase pyridine[24].

Now we discuss the difference among the spectra of porphyrins. The observed ionization potentials (I_{th}^{s}) in solid phase were 5.3, 5.3, and 6.0 eV for ZnTPP, H_2TPP and H_2T(4-Py)P, respectively. The large value for H_2T(4-Py)P can be explained by the inductive effect of the substituents: electron-withdrawing nature of pyridine causes the increase of the I_{th}^{s} of H_2T(4-Py)P. As concerned with the peak A, there is difference in the degeneracy of the HOMO and the next-HOMO. As seen in the simulated spectra, peak A consists of the two non-degenerate π orbitals in the case of porphine, H_2TPP and H_2T(4-Py)P. On the other hand, peak A of ZnTPP involves doubly degenerate π orbitals. This is due to the difference of the symmetry of the system: In the former case, porhine macrocycle has D_{2h} symmetry with two kinds of nitrogen with and without hydrogen, while it has D_{4h} symmetry with only one kind of nitrogen in the latter case. These results are consistent with the previous work by X-ray photoelectron spectroscopy (XPS)[25]. In the present UPS spectra, the width of peak A of ZnTPP (0.68eV) was found to be about 10% less than those of H_2TPP and H_2T(4-Py)P (0.76eV). This difference may be due to this difference of the degeneracy.

(b) Electronic structures of porphyrin/metal interfaces

(b1) ZnTPP/metal interface

The filled circles in Figure 7 show the UPS spectra in the low binding energy region for ZnTPP/Au, Ag, Al, Mg systems. The film thickness was 5nm. The peak position of the UPS spectra relative to the Fermi level of the metal shows a drastic dependence on the metal substrate. Table 1 summarizes the measured values of work function of the metal (Φ_m), the energy of the onset (threshold) of peak A relative to the Fermi level of metal (ε_v^F), and the energy of the vacuum level of ZnTPP relative to the Fermi level of metal (ε_{vac}^F). The superscript UHV indicates the results measured under the

TABLE 1. Summary of the observed energy parameters (in eV) of ZnTPP/metal interfaces. For definitions, see Fig.1 and text.

	In UHV condition					After exposure to oxygen			
metal	Φ_m	ε_v^F(UHV)	ε_{vac}^F	$\Delta=\varepsilon_{vac}^F-\Phi_m$	I_s^{th}	ε_v^F(OX)	ε_{vac}^F	ε_v^F(OX)- ε_v^F(UHV)	I_s^{th}
Mg	3.8_8	-2.1_0	3.2_3	-0.6_5	5.3_3	-1.8_5	3.5_2	$+0.2_5$	5.3_7
Al	4.3_0	-1.7_3	3.6_3	-0.6_7	5.3_6	-1.9_8	3.3_0	-0.2_5	5.2_8
Ag	4.3_0	-1.7_3	3.6_1	-0.6_9	5.3_4	-1.0_3	4.3_6	$+0.7_0$	5.3_9
Au	4.7_8	-1.1_6	4.2_1	-0.5_7	5.3_7	-1.1_4	4.2_1	$+0.0_2$	5.3_5

UHV (ultra high vacuum) condition. These values did not show notable dependence on the film thickness in the range from 1 to 5 nm.

In Figure 8 the values of ε_v^F and ε_{vac}^F of the ZnTPP films are plotted versus Φ_m. These plots show good linear relations. The lines by least-squares fit in Fig. 8 are $\varepsilon_{vac}^F = 1.09\Phi_m - 1.05$ and $\varepsilon_v^F = 1.04\Phi_m - 6.21$ (in eV), with correlation coefficients of almost unity (0.995 for both ε_{vac}^F and ε_v^F). These results indicate that the energies of the levels of ZnTPP are linear function of Φ_m with a slope of almost unity. We will compare these results with expectations from the traditional models in Fig.1. If Fermi-level alignment occurs (Fig.1(a)), ε_v^F should be constant irrespective of the substrate, and we expect flat lines in Fig.8. On the other hand, if vacuum-level alignment occurs (Fig.1(b)), $\Delta = \varepsilon_{vac}^F - \Phi_m$ should be equal to zero, and we expect $\varepsilon_{vac}^F = \Phi_m$ in Fig.8. The presently observed results show that neither of these cases holds at the ZnTPP/metal interfaces. In Figure 9, we plot Δ as a function of Φ_m. As seen in the figure, the observed energy shift of the vacuum levels at the interface is almost constant ($\Delta \cong 0.7$ eV) irrespective of Φ_m. These findings indicate that the energy

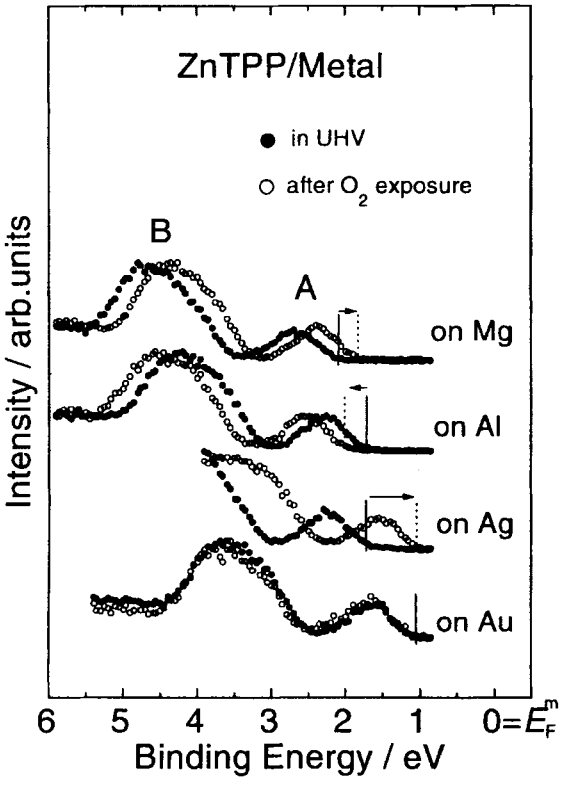

FIGURE 7.
UPS spectra in the uppermost valence region for ZnTPP films evaporated on various metals (Mg, Al, Ag, Au) in ultrahigh vacuum (filled circles) and after exposure to oxygen (open circles). The solid and dotted vertical lines indicate the onset of peak A measured before and after exposure to oxygen, respectively. The energy shift by exposure to oxygen is denoted by an arrow.

levels of ZnTPP align with those of the substrate metal with a finite constant shift of the vacuum level, as shown in Fig.1(c). Similar abrupt shift of vacuum level at the organic/inorganic interface was observed for merocyanine dye/Ag halide interfaces[26]. This shift indicates the formation of an electric double layer at the interface. Since all porphyrins studied have no permanent dipole, this dipole layer should be the result of electronic rearrangement at the interface. The constant magnitude of Δ suggests that the interaction is not due to chemical bonding but electrostatic interaction (e.g. image potential) near the interface. This, however, needs further experimental examination. The apparent lack of band bending within the film thickness of 5nm may be explained by the low carrier density of well-purified ZnTPP, which leads to small slope of band bending and a very large thickness of the space charge layer.

Next we examine the effect of exposure to oxygen. The open circles in Figure 7 show the UPS spectra in the low binding energy region of ZnTPP/Au, Ag, Al, Mg specimen after exposure to 1.2×10^9 L oxygen (4 Torr, 5 minutes; $1L=10^{-6}$ Torr · s) and subsequent evacuation to UHV region. The spectral lineshape is still similar to that observed in the UHV condition, suggesting only weak interaction between ZnTPP and oxygen, but the energy position of the spectral features are different from that in the UHV condition. As shown in Table 1 (the superscript OX indicates the results measured after oxygen exposure) the extent and direction of the energy shift are strongly dependent on the substrate (see $\varepsilon_v^F(OX) - \varepsilon_v^F(UHV)$ in Table 1). This variation cannot be ascribed to the doping of ZnTPP by oxygen alone, since this should lead to a constant shift irrespective of the substrate metal.

Rather, this behavior can be explained by the change of the work function of the substrate metal by oxygen. It is plausible that oxygen reaches the interface through defects and grain boundaries of ZnTPP film and interacts with the metal surfaces. It is known that the work function of most metal surface is increased by the exposure to oxygen due to the large electronegativity of oxygen atom. On the other hand, the work function of Au surface is insensitive to oxygen exposure due to its chemical stability[27] and that of Al surface is slightly decreased by oxygen exposure due to unusual surface structure of its oxidized surface[28]. This trend of work function change qualitatively corresponds to the observed shift $\varepsilon_{vac}^F(OX) - \varepsilon_{vac}^F(UHV)$, which strongly supports the idea that the energy levels of ZnTPP are aligned with the vacuum level of the metal substrate. The very small shift of the UPS of ZnTPP on Au suggests that the shift by the oxygen-doping is negligibly small.

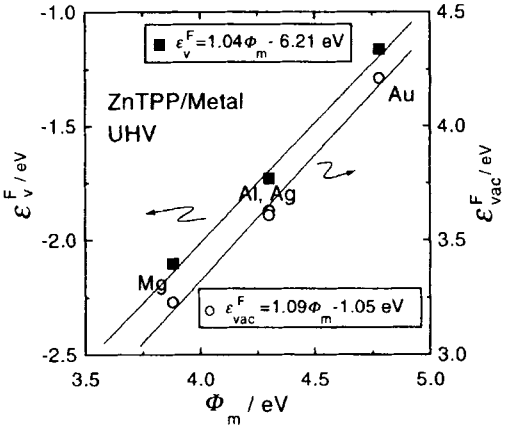

FIGURE 8.
Plots of the energies of the onset of peak A (ε_v^F) (■) and the vacuum level of ZnTPP (ε_{vac}^F) (○) against the work function of metal (Φ_m). The least-squares straight lines are also indicated.

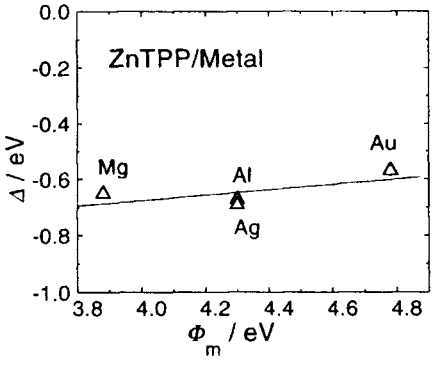

FIGURE 9.
Plot of the vacuum level shifts (Δ) at ZnTPP/metal interfaces against the work function of metal (Φ_m).

(b-2) H_2TPP/metal and H_2T(4-Py)P/metal interfaces

For H_2TPP and H_2T(4-Py)P, we performed similar experiments as those for ZnTPP. The observed energy parameters are listed in Table 2. In Figs.10(a) and 10(b), we plot ε_{vac}^F and ε_v^F of H_2TPP and H_2T(4-Py)P films (5nm thick) versus Φ_m with the results of ZnTPP/metal interfaces. These plots show also good linear relations. In contrast to ZnTPP/metal interfaces, the slope of the plots is not unity but about a half. Figure 10(c)

shows the plots of Δ against Φ_m. The shift of the vacuum level at the interface (Δ) is not zero, indicating that the concept of a common vacuum level is again invalid for these interfaces, as in the case of ZnTPP. These results suggest that the energy levels of $H_2T(4\text{-Py})P$ and H_2TPP are also fixed to the vacuum level of the substrate metal with an energy shift Δ. In contrast to the case of ZnTPP/metal systems, however, Δ is not constant, but a linear function of Φ_m.

Such linearity of level-energy against metal work function has been observed for inorganic semiconductor/metal system[29]. A slope parameter which is defined as $S \equiv d\phi_B/d\phi_m$ (ϕ_B is the Schottky barrier height) is known to depend on the type of the semiconductor. S corresponds to the slope of the ε_v^F versus Φ_m plot in our discussion. When Schottky-Mott rule holds, i.e. there is no interface state at the interface (Schottky

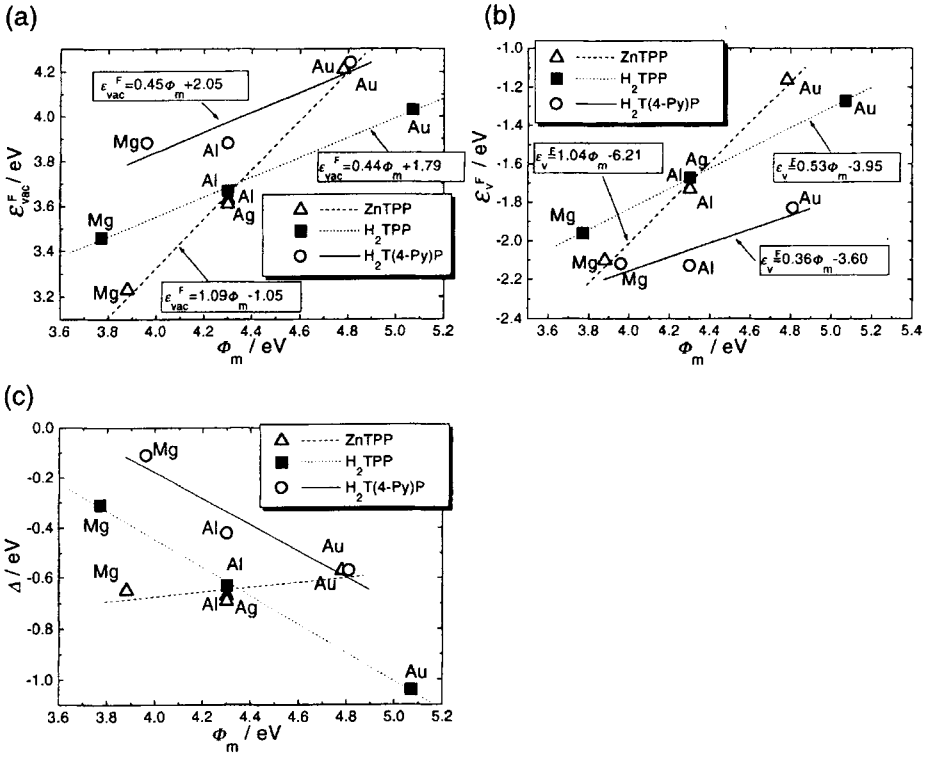

FIGURE 10.
Plots of the observed energy parameters against the work function of metal (Φ_m) for ZnTPP(△), H_2TPP(■), and $H_2T(4\text{-Py})P$(○). (a) plots of the energies of the onset of peak A (ε_v^F) against Φ_m, (b) plots of the energy of the vacuum level of the porphyrin film (ε_{vac}^F) against Φ_m, and (c) plots of the vacuum level shifts (Δ) against Φ_m. The least-squares straight lines are also indicated.

limit), the value of S should be unity. On the other hand, when there is interface states which has sufficient densities to pin the Fermi level of the semiconductor, it should be zero (Bardeen limit). The reported values of S in most inorganic-semiconductor/metal junction are between zero and unity[29]. For example, S is about 0.1 for Si, GaAs and Ge, and about 0.5 for compound semiconductor such as ZnSe and ZnS[30], suggesting the effect of the interface states. The small slope for $H_2T(4\text{-Py})P$ and H_2TPP /metals systems may be also explained by similar effect of the interface states. Although no intrinsic interface state is known for organic solids, possible extrinsic interface states such as defect states, impurity levels, and metal-induced gap state (MIGS)[29] may be responsible for the observed behavior. Possible origins of such variety in S among the porphyrins may be (i) higher purity of ZnTPP due to additional DDQ treatment, and (ii) the existence of the central metal which may affect the nature of the interaction between the metal surface and the first porphyrin layer. Further study is necessary to clarify this point.

Finally we discuss the relation between the observed electronic structure and the conduction type. The observed ionization potentials (I_{th}^{s}) in the solid phase were 5.3, 5.3, and 6.0 eV for ZnTPP, H_2TPP and $H_2T(4\text{-Py})P$, respectively. $H_2T(4\text{-Py})P$, which is known to be n-type, has larger I_{th}^{s} than ZnTPP and H_2TPP with p-type character. A similar correlation between I_{th}^{s} and the conduction type was reported for phthalocyanine derivatives[10]. For H_2TPP and $H_2T(4\text{-Py})P$, PM3 calculations gave almost the same pattern of wave functions for the frontier orbitals, which are expected to dominate the electric properties as well as conduction type. These results indicate that the change of the conduction type of porphyrins by substitution is not accompanied with an essential change of the frontier orbitals except for their energy position. Here we discuss the conduction type on the basis of the observed interfacial electronic structures.

As seen in Fig.10(b), the energy of the HOMO relative to Fermi level of the metal substrate (ε_v^F) strongly depends on both the metal work function and the organic compound. At first we focus on the results for Au substrate. The values of ε_v^F for Au are -1.1_6, -1.2_7, and -1.8_3 eV for ZnTPP, H_2TPP, and $H_2T(4\text{-Py})P$, respectively. If we regard the optical excitation energy (2.08 eV for ZnTPP, 1.92 eV for H_2TPP and $H_2T(4\text{-Py})P$[31]) as the band gap (the actual band gap may be slightly larger, since this assumption ignores excitonic effect), the Fermi level of the Au substrate is around the center of the gap for ZnTPP and H_2TPP, while it is very close to the LUMO for $H_2T(4\text{-Py})P$. Thus we can expect strong electron-injecting nature for the $H_2T(4\text{-Py})P$/Au interface in contrast to the other interfaces. This expectation is consistent with the

observed carrier-injecting character by displacement current measurement[32]. If we classify the conduction type by the carrier-injecting character, the position of the frontier orbital at the interface well correlates with the conduction type. On the other hand, for metals with low work functions, especially for Mg substrate, there is little difference in the energy position of the HOMO (ε_v^F) among the porphyrins irrespective of the "conducting type" assigned from the results for the interfaces with Au. For all the porphyrin/Mg interfaces, electron-injecting nature can be expected, with little correlation between the interfacial electric properties and the "conduction type". These results strongly suggest that the "conduction type" of an organic semiconductor from interface-related electrical measurements should be dependent on the electrode metal used in the experiments. For further clarification of these points, the investigation of the space charge layer and the determination of the Fermi level of the organic semiconductor will be necessary.

TABLE 2. Summary of the observed energy parameters (in eV) for H_2TPP and $H_2T(4\text{-Py})P$/metal interfaces. For definitions, see Fig.1 and text.

H_2TPP					
metal	Φ_m	ε_v^F	ε_{vac}^F	$\Delta=\varepsilon_{vac}^F-\Phi_m$	I_s^{th}
Mg	3.7_7	-1.9_6	3.4_6	-0.3_1	5.4_2
Al	4.3_0	-1.6_7	3.6_7	-0.6_3	5.3_4
Au	5.0_7	-1.2_7	4.0_3	-1.0_4	5.3_0

$H_2T(4\text{-Py})P$					
metal	Φ_m	ε_v^F	ε_{vac}^F	$\Delta=\varepsilon_{vac}^F-\Phi_m$	I_s^{th}
Mg	3.9_6	-2.1_2	3.8_8	-0.1_1	6.0_0
Al	4.3_0	-2.1_3	3.8_8	-0.4_2	6.0_1
Au	4.8_1	-1.8_3	4.2_4	-0.5_7	6.0_7

SUMMARY

The electronic structures of porphyrins and their interfaces with various metals were investigated using ultraviolet photoemission spectroscopy in order to examine (i) bulk electronic structure, (ii) the energy level alignment at the porphyrin/metal interfaces and (iii) the relation between the electronic structure and the conduction type of

porphyrins.

The observed valence electronic structures of the porphyrins can be regarded as the superposition of those of porphine and the substituents. The energy levels of the porphyrins relative to the Fermi level of substrate metals could be expressed as linear functions of the work function of metals with the shift of the vacuum level at interface (Δ). This indicates that the energy levels of the porphyrins align to the vacuum level of the substrate metal with the vacuum level shift due to interfacial dipole, clearly implying the invalidity of the assumption of "a common vacuum level". The slope of the linear functions was about unity for ZnTPP, indicating that the extent of Δ is constant for ZnTPP/metal. For H_2TPP and H_2T(4-Py)P, the slope was much smaller than unity, indicating that Δ is also a linear function of Φ_m. This deviation of the slope from unity suggests the existence of interface states.

These findings strongly indicate the necessity of the modification of the traditional model of the energy level alignment at the organic/metal interface. Especially, the traditional method for the estimation of the interfacial electronic structure has possibility to predict incorrect electric properties of the interface, since the magnitude of the observed Δ (upto -1.0eV) is comparable with the band gap. For a deeper insight into the mechanism of energy level alignment, it is important to clarify the origin of the interfacial dipole based on the interaction between the metal surface and the organic layer.

The ionization potential of H_2T(4-Py)P was 0.7eV larger than those of H_2TPP and ZnTPP due to the inductive effect of pyridyl-group of electron-withdrawing nature. This tendency of the ionization potentials well corresponds with the conduction type reported for phtahlocyanine-derivatives[10]. For porphyrin/Au interface, the energy position of the frontier orbitals relative to the Fermi level of the Au substrate exhibits good correlation with the conduction type. However, the correspondence was poor for the other interfaces with low work function metals. In order to establish truly meaningful concept of this type, it is necessary to understand the mechanism of the interfacial electric process by which the conduction type is judged.

DEDICATION

It is our great pleasure to dedicate this article to Professor Yusei Maruyama and Professor Fumio Ogura who have been active in the field of electrically and electronically functional organic materials on the occasion of their retirement.

ACKNWLEDGMENT

We thank Professor Yoshio Uemori of Kanazawa Technical University for the instructions about DDQ treatment, and Drs. Shun Egusa and Takashi Sasaki of Toshiba R&D Center for helpful discussion. This work was supported in part by Grant-in-Aids for Scientific Research from the Ministry of Education, Science, and Culture of Japan (Nos. 04403001, 07NP0303, 07CE2004) and the Venture Business Laboratory Program "High Performance Nanoprocesses" at Nagoya University. This work was performed as a Joint Studies Program of the UVSOR facility of Institute for Molecular Science (No.6-H217).

REFERENCES

1. For reviews, see for example, (a) J.Simon, J. J. Andre, Molecular Semiconductors (Springer-Verlag, Berlin, 1985). (b) N. C. Greenham and R. H. Friend, Solid State Phys., 49, 1 (1995).
2. T. R. Ohno, Y. Chen, S. E. Harvey, G. H. Kroll, J. H. Weaver, R. E. Haufler, and R. E. Smalley, Phys. Rev., B44, 13747(1991).
3. W. R. Salaneck, and J. L. Brédas, Adv. Mater., 8, 48 (1996).
4. S. Narioka, H. Ishii, D. Yoshimura, M. Sei, Y. Ouchi, K. Seki, S. Hasegawa, T. Miyazaki, Y. Harima, and K. Yamashita, Appl. Phys. Lett., 67, 1899 (1995).
5. Y. Hirose, A. Kahn, V. Aristov, and P. Soukiassian, Appl. Phys. Lett., 68, 217 (1996).
6. W.Schottky, Phys. Z., 41, 570 (1940). N. F. Mott, Proc. Cambridge Phil. Soc., 34, 568 (1938).
7. J. Simon, J. J. Andre, Moleular Semiconductors (Springer-Verlag, Berlin, 1985).
8. K. Yamashita, Y. Harima, and T. Matsubayashi, J. Phys. Chem., 93, 5311 (1989).
9. D. Wöhrle, and D. Meissner, Adv. Mater., 3, 129 (1991).
10. D. Schlettwein, and N. R. Armstrong, J. Phys. Chem., 98, 11771 (1994).
11. J. H. Fuhrhop and K. M. Smith (Eds), Porphyrins and Metalloporphyrins (Elsevier, N.Y. 1975).
12. K. Seki, H. Nakagawa, K. Fukui, E. Ishiguro, R. Kato, T. Mori, K. Sakai, and M. Watanabe, Nucl. Instrum. Methods, A246, 264 (1986).
13. J. H. Fomenko, in Handbook of Thermoionic Porperties, edited by G. V. Samsonov (Plenum, New York, 1966).
14. J. J. P. Stewart, QCPE Bull., 3, 43 (1983).
15. J. J. P. Stewart, J. Comput. Chem., 10, 209 (1989).
16. C. B. Duke, A. Paton, and S. R. Salaneck, Mol. Cryst. Liq. Cryst., 83, 177 (1982), and references therein.
17. P. Dupuis, R. Roberge and C. Sandorfy, Chem. Phys. Lett., 75, 434 (1980).
18. K. L. Yip, C. B. Duke, W. R. Salaneck, E. W. Plummer and G. Loubriel, Chem. Phys. Lett., 49, 530 (1977).
19. E. Orti, J. L. Brédas, Chem. Phys. Lett., 164, 247 (1989).
20. A.Ghosh, J. Almlöf and P. G. Gassman, Chem. Phys. Lett., 186, 113 (1991).
21. D. Spangler, G. M. Maggiora, L. L. Shipman and R. E. Christoffersen, J. Am. Chem. Soc., 99, 7470 (1977).
22. L. Asbrink, O. Edqvist, E. Lindholm, and L. E. Selin, Chem. Phys. Lett., 5, 192 (1970).
23. E. E. Koch, M. Iwan, K. Hermann and P. S. Bagus, Chem. Phys., 59, 249 (1981).
24. K. Kimura, S. Katsumata, Y. Achiba, T. Yamazaki and S. Iwata, Handbook of He I

Photoelectron Spectra of Fundamental Organic Molecules (Japan Scientific Societies Press, Tokyo, 1988).
25. M. V. Zeller and R. G. Hayes, J. Am. Chem. Soc., 95, 3855 (1973).
26. K. Seki, H. Yanagi, Y. Kobayashi, T. Ohta, and T. Tani, Phys. Rev., B49, 2760 (1994).
27. V. A. Sobyanin, V. V. Gorodetskii and N. N. Bulgakov, React. Kinet. Catal. Lett., 7, 285 (1977).
28. U. Memmert and P. R. Norton, Surf. Sci., 203, L689 (1988).
29. R. Mönch, Surf. Sci,. 299/300, 928 (1994). and references therein.
30. S. Kurtin, T. C. McGill and C. H. Mead, Phys. Rev. Lett., 22, 1422 (1969).
31. E. B. Fleischer, A. M.Shachter, Inorg. Chem., 30, 3763 (1991).
32. S. Egusa, T. Sasaki, Molecular Electronics and Bioelectronics, 6, 68 (1995) (in Japanese).
On displacement current measurement, see K. Yamamoto, S. Egusa, M. Sugiuchi, and A. Miura, Solid State Commun., 85, 5 (1993).